

Article

Fabrication Temperature-Related Porosity Effects on the Mechanical Properties of Additively Manufactured CFRP Composites

Olusanmi Adeniran ^{1,*}, Norman Osa-uwagboe^{2,3}, Weilong Cong ¹ and Monsuru Ramoni ⁴

¹ Department of Industrial, Manufacturing, and Systems Engineering, Texas Tech University, Lubbock, TX 79409, USA.

² Wolfson School of Mechanical, Electrical, and Manufacturing Engineering, Loughborough University, Loughborough, Leicestershire LE11 3TU, UK

³ Air Force Research and Development Centre, Nigerian Air Force Base, Kaduna, PMB 2104, Nigeria.

⁴ Department of Industrial Engineering, Navajo Technical University, Crownpoint, NM 87313, USA.

* Correspondence: Olusanmi.adeniran@ttu.edu; Tel.: +1(682)-561-4015

Abstract: The use of additive manufacturing in fabricating composite components has been gaining traction in the past decade. However, some issues with mechanical performance still need to be resolved. The issue of material porosity remains a pertinent one that needs more understanding to be able to determine viable solutions. Different researchers have examined the subject of porosity issues in additively manufactured (AM) carbon-fiber-reinforced-plastic (CFRP) composites. However, more research to quantitatively determine the effects of fabrication temperatures at the micro-scale is still needed. This study employed micro CT scan analysis to quantitatively compare the effects of fabrication temperatures at 230°C, 250°C, 270°C, and 290°C for carbon-fiber-reinforced polyamide (CF-PA) and carbon-fiber-reinforced acrylonitrile-butadiene-styrene (CF-ABS) composites. This followed an SEM evaluation which was used to determine the effects of the temperatures on interlayer and intralayer porosity generation. The porosity volume was related to the mechanical properties results in which it was determined how deposition temperatures affect the porosity volumes. It was also determined that semicrystalline composites are generally more affected by fabrication temperatures than amorphous composites, with the relationship between porosity and mechanical properties also established. The overall porosity volume from the interlayer and intralayer voids was also determined, with the interlayer voids found to play a more determinant role in influencing the mechanical properties.

Keywords: additive manufacturing; fabrication temperature; porosity effects; carbon-fiber-reinforced polymer composites; mechanical properties; micro CT scan

1. Introduction

1.1. Additively Manufactured CFRP Composites

The rapid increase in demand for products with a diversity of applicability, accuracy, and ease of manufacture has led to the advancement of flexible manufacturing techniques. The concept of AM has grown in the last two decades into a reliable method of producing complex structures for several industrial applications such as aerospace, biomedical, automobile, telecommunications, defense, and renewable energies [1]. This expansive application could be traced to the advantage of manufacturing prototypes quickly at lower costs and without specialized tooling [2–4].

A distinguishing feature of CFRP composite fabrication by AM interlayer features of the fabrication method. This contributes immensely to the degree of porosity in the material to determine its mechanical performance. The interlayers are characterized by relatively large triangular voids of similar sizes which are formed as gaps between the print beads during deposition. This often compounds the issue of porosity, resulting in lower

mechanical properties than parts fabricated through other manufacturing methods. Hence, the importance of a better understanding of fabrication temperature influenced interlayer and intralayer porosity effects. To advance the art of the manufacturing technique, more understanding of process parameter effects is still needed to improve the viability of the manufacturing method.

1.2. Current understanding of deposition temperature-related porosity effects in AM fabricated CFRP composites.

Different studies have conducted investigations on porosity effects on the mechanical performance of AM-fabricated CFRP composites [5–12]. However, there are still limited investigations on the quantitative comparison of fabrication temperature-related porosity effects. A better understanding provided by the degree of details of micro CT analysis is still needed to further knowledge cultivation on how deposition temperatures influence porosity features and affect the mechanical performance of AM-fabricated CFRP composites. The investigations that examined porosity effects did not evaluate deposition temperature effects, and the ones that examined temperature effects did not qualitatively compare porosity effects.

Zhang et al. [5] examined interlayer porosities as influenced by printing raster angles in AM-fabricated CFRP composites but did not consider the effects of deposition temperatures. Petro et al. [9] explored an X-Ray CT scan to determine porosity volumes in a 41% fiber content continuous CFRP composite, where they compare the results to that tested to the ASTM D3171 standard. However, they did not consider fabrication temperature-related porosity effects. Tekinalp et al. [6] investigated the effect of fiber volumes on tensile properties and the degree of porosity. However, they did not examine the effect of printing temperatures nor provided a clear measurement procedure to arrive at their reported porosity values. Ning et al. provided porosity measurements in two of their reported investigations [7,13] which examined the effects of fiber content and the effects of reinforcement materials on porosities. However, they applied a rudiment measurement procedure, where they applied manual weighing of samples and subtraction from a calculated solid mass. In their other study [14], where they tested the effects of process factors including fabrication temperatures, they did not measure or compare porosities volumes.

Other reported investigations on the effects of process temperatures on the mechanical performance of AM-fabricated CFRP composites have been devoted to layer strength from matrix material viscoelasticity fluidity rather than addressing the topic of temperature-related porosity effects [15–19]. Ajinjeru et al. [15] investigated the viscoelasticity of polyetherimide (PEI) matrix at process temperature to gain more understanding of matrix material fluidity effects on the ease of processing but did not examine porosity effects. The researchers also investigated acrylonitrile-butadiene-styrene (ABS) and Polyphenyl sulfone (PPSU) to determine suitable processing conditions [20], but also did not investigate porosity. Kishore et al. [17] investigated interlayer strength improvement by using infrared heating to increase the surface temperature of the printed layer just before the deposition of the succeeding layer, thus, improving surface properties. However, they did not examine temperature-influenced porosity. Yang et al. [19] investigated a novel process consisting of continuous fiber hot-dipping, matrix material melting, and impregnated composite extrusion to improve composite properties, but did not discuss the topic of temperature-related porosity effects.

1.3. Research motivations

Of all the determined challenges to the successful application of AM-fabricated CFRP composites, the issue of interlayer and intralayer porosity is one of the pertinent which need better understanding. Yet, a detailed quantitative understanding of printing temperature-influenced porosity effect on the mechanical performance of the composites is not well developed. This motivated this study to investigate printing temperature-related porosity effects on the mechanical performance of the composite for samples fabricated

using the fused deposition modeling (FDM) technique. The investigations included evaluating the relationships between printing temperatures, mesostructure formation, fabrication porosities, and the mechanical properties of the composite. The understanding gained would help contribute to knowledge in the fabrication temperature process control for the improved mechanical performance of CFRP composites fabricated AM.

2. Materials and Methods

2.1. AM Workpiece Fabrication Procedure

Test workpieces used to conduct the investigations were fabricated from two different CFRP composite materials with manufactured carbon fiber averages of 7 μm diameter and less than 400 μm length: 15% CF-PA6 filament compounded from high-modulus short carbon fiber in a PA6 copolymer (3D XTEC, Grand Rapids, MI, USA), and 15% CF-ABS filament compounded from high-modulus short carbon fiber in Sabic MG-94 ABS (3D XTEC, Grand Rapids, MI, USA).

A 3D printer (Prusa Mk3 i3, Prague, Czech Republic) was used for the FDM fabrication in a modified control printing enclosure fixture (Creality 3D, Shenzhen, China) to maintain a $45 \pm 5^\circ\text{C}$ printing environment temperature and relative humidity of lower than 20% RH. The $230^\circ\text{C} - 290^\circ\text{C}$ printing temperature range was chosen to determine how fabrication temperatures influence porosity volume because of the material viscosities and flowability within those temperatures range. Table 1 shows the printing parameters used to fabricate the test workpieces while Figure 1 illustrates the 3D printer setup employed.

Table 1. Material Processing Parameter.

Parameter	Unit	Value
Infill Density	%	100
Printer Enclosed Temperature	$^\circ\text{C}$	50 ± 5
Bed Temperature	$^\circ\text{C}$	100
Raster Angle	Deg	0, 90
Layer Thickness	mm	0.25
Printing Speed	mm/sec	30
Nozzle Temperature	$^\circ\text{C}$	230, 250, 270, 290

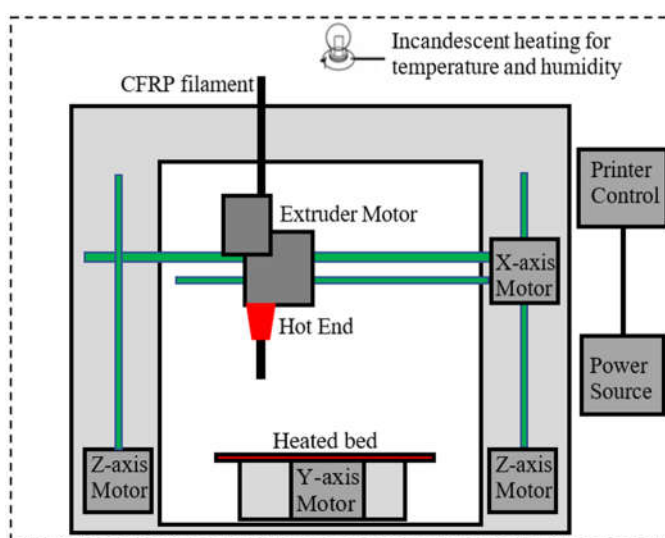


Figure 1. 3D Printer setup to control immediate printing environment temperature and humidity. Based on Adeniran et al. [21.]

2.2. Measurement Procedure

2.2.1. Mechanical measurements

Tensile samples which consisted of four workpieces each per data point for the AM-fabricated CF-PA and CF-ABS composites were tested to quantitatively compare fabricating temperature-related porosities and the resulting effects on the mechanical properties of the composites. A 10 kN load cell in a universal mechanical tester (MTS Criterion Model 45, Eden Prairie, MN, USA) was used to conduct tensile tests, while a 10 kg minor load and 100 kg major loads were used in the Rockwell tester (Clark C12A, Novi, MI, USA) to conduct the hardness test. Table 2 shows the test procedures applied in the study.

Table 2. Test Standard and Equipment.

Test	ASTM Standard	Equipment	Test Speed	Unit
Tensile	D638 (Type I)	MTS Criterion Model 45	5.0	mm/min
Rockwell Hardness	D785	Clark Tester C12A	-	-
Scanning Electron Microscopy	-	Thermo Scientific Phenom XL	100X	Magnification
Micro-CT	-	Nikon X-Tex XTH	1000	mm

2.2.2. Scanning Electron Microscopy

Cross-sections of fractured tensile workpieces of the CF-PA and CF-ABS samples printed at 230°C, 250°C, 270°C, and 290°C were examined at 100X magnification in a Scanning Electron Microscope (Thermo Fisher Phenom XL, Waltham, MA, USA) to evaluate the mesostructure formation of the composites as determined by the deposition temperature and matrix materials.

2.2.3. Micro-CT Microscopy

To improve the accuracy of the temperature influenced-porosity determination, 3 samples each with cross-section volumes of 25 mm x 9 mm x 2.5 mm were scanned for each data point of the 230°C, 250°C, 270°C, and 290°C composite samples. Each cross-sectional volume was divided into 6 segments as illustrated in Figure 2 with the average mean porosity values determined over the segmented volumes while Figure 3 shows the micro CT microscope (Nikon XTH X-Tex 160Xi, France) configuration used for the measurement.

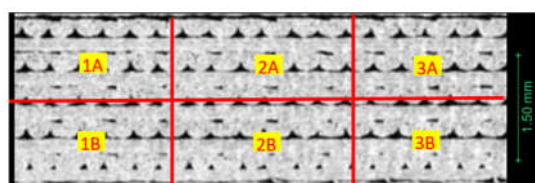


Figure 2. Illustration of segmented volume areas used in Micro-CT porosity determination of AM fabricated CFRP composites.

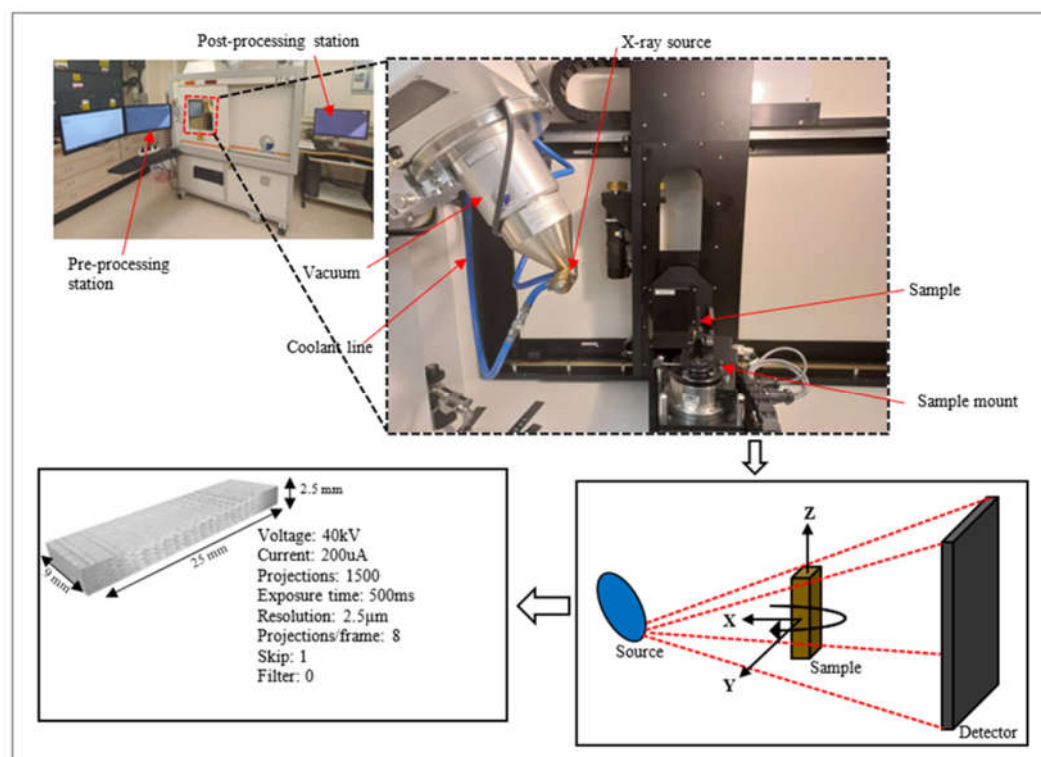


Figure 3. X-ray micro-CT setup and detailed scanning parameters.

The scan was performed on the CT scan microscope with the scanning point-to-point resolution set to $2.5\mu\text{m}$ at exposure times of 500 ms with a total of 3016 tiff images created per sample scan. The acquired microscopy data were transferred and post-processed using commercial software (Dragonfly ORS, Adelaide, South Australia, Australia). The automatic feature of the software was used to determine the optimum center of rotation, with all generated slices combined to develop the volumetric image in the reconstruction phase. Characterization noise generated with the volumetric imaging was reduced using Gaussian filters, which in the case of this investigation experienced minimal data loss from the sample materials' homogeneity. The generated tiff files were incorporated into the software with voxel analysis to determine volumetric porosity. Figure 3 shows the test equipment with an illustration of the imaging process.

3. Results

3.1. Scanning electron microscopy results

SEM determination was used to interpret the $230\text{ }^{\circ}\text{C}$ to $290\text{ }^{\circ}\text{C}$ printing temperature effects on interlayer and intralayer porosity generation for the composites. The thermal history of adjoining melt layers as determined by deposition temperatures influences the extrusion melt solidification, bonding, and the interlayer feature formed including the degree of porosity.

3.1.1. SEM result for CF-PA composite

Figure 4 shows the SEM observation of the mesostructure features for the AM-fabricated CF-PA composites.

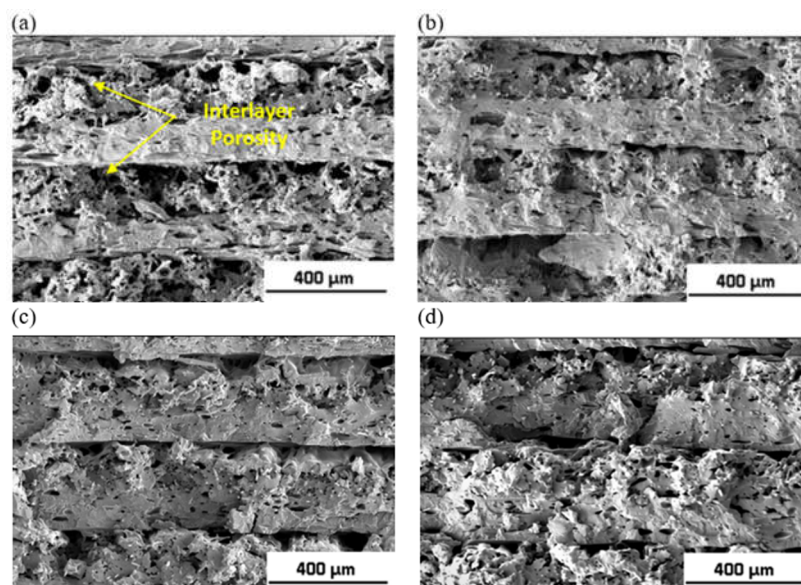


Figure 4. Mesostructure of CF-PA composites printed at (a) 230°C (b) 250°C (c) 270°C (d) 290°C [100X].

The SEM examination of AM-fabricated CF-PA composite shows increasing fiber-matrix coalescence with nozzle head temperatures for the 230 °C – 290 °C temperature range examined. A spongy-like mesostructure with less regular layer formation was observed, which can be attributed to the excessive shrinkage from the semicrystalline matrix recrystallization on cooling down from fabrication. The low melt viscosity of the semicrystalline morphology can also be ascribed to contributing to the irregular interlayer mesostructure formation, with porosity also likely issues. According to Vaes and Puyvelde [22], porosities could be an issue in semicrystalline matrix AM fabrication due to the heterogenous self-nucleation of their structural crystals from insufficient heat transfer, melting, and high shear deformations during fabrication to influence the material's porosities.

The fusion bonding theory applies to AM composite fabrication, where the increasing heat from the 230°C – 290°C nozzle head temperatures in this case improved the carbon-fiber-matrix coalescence to reduce interlayer porosities. This is because the higher the fabrication temperature above the glass transition temperature, the more evenly the mechanisms of chain rearrangement in the print during the heating and solidification process [23].

3.1.2. SEM result for CF-ABS composite

Figure 5 shows the SEM observation of the mesostructure features for the AM-fabricated CF-ABS composites.

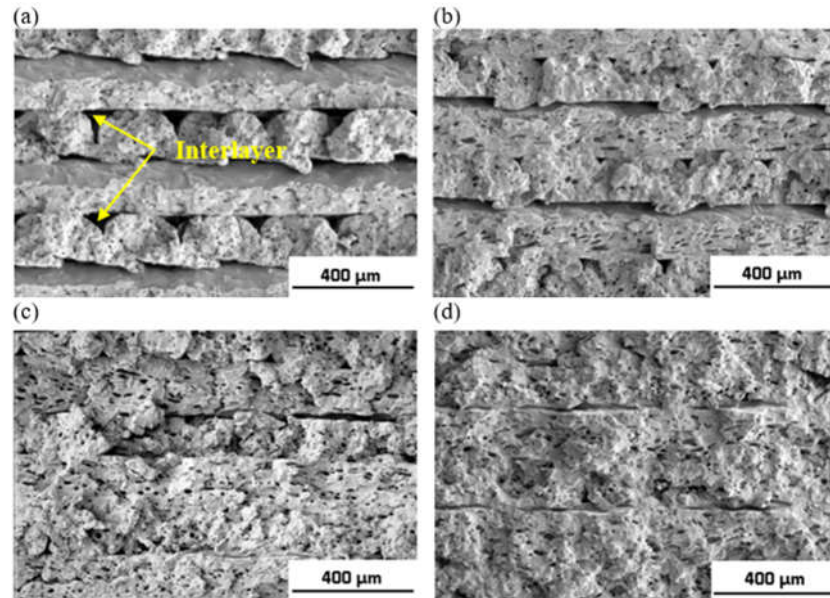


Figure 5. Mesostructure of CF-ABS composites printed at (a) 230°C (b) 250°C (c) 270°C (d) 290°C [100X].

The SEM evaluation in Fig. 5 shows the CF-ABS composite exhibits a regular arrangement of the interlayers in the mesostructure formation. This is because of the high fluidity of the ABS matrix during solidification [24]. Increasing the fabrication temperatures between 270°C – 290°C showed improving mesostructure formation and reduced interlayer porosities that are attributed to improving melt flow with the increased temperatures. However, the higher temperature gradient on cooling down due to the higher temperatures resulted in more intralayer porosities.

Similar to Figure 4, plastic material fusion bonding theory can also be applied to explain how increasing heating from nozzle head temperatures can improve carbon-fiber-matrix coalescence and reduce interlayer porosities in the CF-ABS composites. However, at a (more elevated) temperature, increasing temperature becomes detrimental, which could result in degraded molecular chain strength, resulting in reduced mechanical performance, as was seen with the 290°C fabrication temperature for the composite.

3.2. Micro CT-scan result

The micro CT scan provides a more detailed quantitative evaluation of porosity features. Through the scan, porosity volume comparison for the different fabrication temperatures was determined. Figure 6 shows reconstructed CT scan void images for the CF-PA and CF-ABS composites, which shows a general void reduction with the increasing fabrication temperature under study.

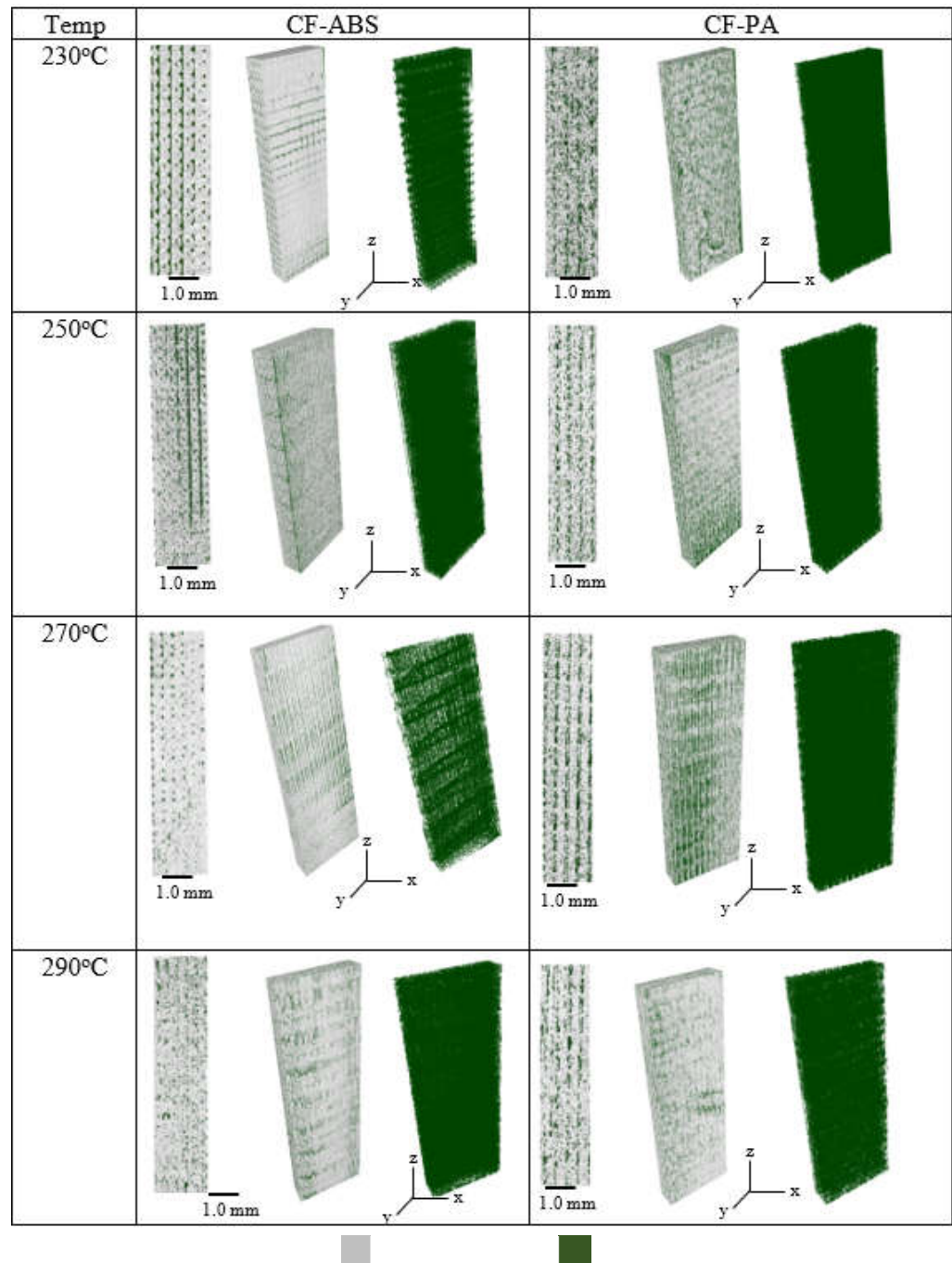


Figure 6. Reconstructed X-ray CT void for CF-ABS and CF-PA composite specimens for the different fabrication temperatures under study.

The variation could be visualized with the grey pixels representing the solid volume of the composite while the green pixels represent the porosities. Understanding fabrication temperature effects on the degree of porosity are vital to characterizing the composites' mechanical performance to gain insights into how they affect material properties such as strength, modulus, ductility, toughness, hardness, etc. This is needed to determine the range of fabrication temperatures required to achieve the required material properties for different applications. Figures 7 and 8 show a plot of the test results for the CF-PA and CF-ABS composites, respectively, fabricated at 230°C to 290°C.

3.2.1. Micro CT-scan porosity results for CF-PA composite

The results show an overall reduced porosity trend from the combined inter and intra-layer porosities effect with the increasing 230°C to 290°C fabrication temperatures.

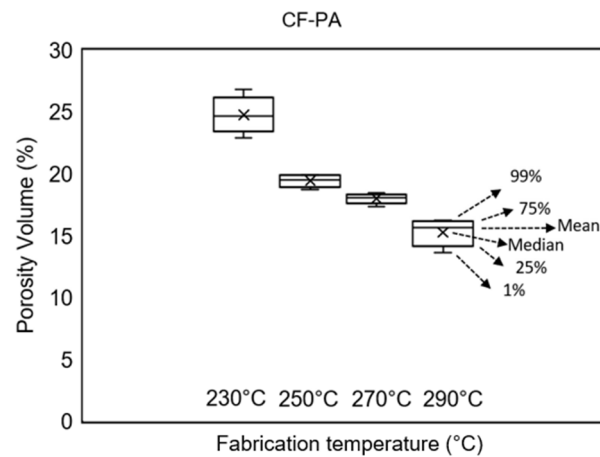


Figure 7. Fabrication temperature-related porosity volume in AM-fabricated CF-PA composite.

Fig. 7 shows a gradual decrease in the porosity of the CF-PA composite as the fabrication temperature increased from 230 °C to 290 °C, with a plot of test data distribution in percentiles within the overall data set. The composites show a consistent reduction in porosity volumes with mean values of 24.7%, 19.4%, 18.0%, and 15.3% for the 230 °C, 250 °C, 270 °C, and 290 °C, respectively. The reduced porosity with the increasing temperature observed was due to the fiber matrix's increasing coalescence, resulting in more solid mesostructure formation of reduced interlayer features.

3.2.2. Micro CT-scan porosity results for CF-ABS composite

Figure 8 shows the results for the overall porosity trends for the CF-ABS within the 230°C to 290°C fabrication temperatures range under study.

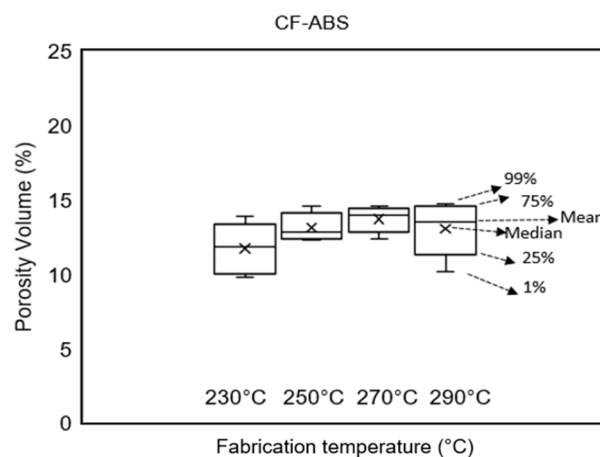


Figure 8. Fabrication temperature-influenced porosity volume in AM-fabricated CF-ABS composite.

Even though the SEM evaluations of the composite showed pronounced interlayer porosity with fabrication temperatures, the effect on the overall porosity volume for the amorphous CF-ABS was not quite pronounced when quantitatively compared in the CT scan measurement. Figure 8 shows the overall porosity volume differences were insignificant at mean values of 11.7 % for the 230 °C, 13.1 % for the 250°C, 13.9 % for the 270 °C, and 13.1 % for the 290 °C samples. Increasing deposition temperature over 230°C to 290°C resulted in more interlayer coalescence with reducing interlayer porosities. However,

increased intralayer porosities as a result of the higher temperature gradient on cooling down. These overall effects from the inter and intra layers were seen to account for the cause of the insignificant differences in the porosity volumes observed across the 230°C to 290°C deposition temperature range under study. The study by Adeniran et. al [25] provided more insight into the porosity types generated in CF-ABS composites fabricated by AM where they discussed two fabrication-generated porosity types. The explained interlayer porosities as triangular gaps in the non-contact areas of the print beads during layer-upon-layer material build-up while intralayer porosities are the void formation inside individual print beads due to gas evolution in the course of the semi-liquid to extrusion of the print material.

3.3. Fabrication temperature-related porosity effects on mechanical properties

3.3.1. Mechanical properties of CF-PA composite

A generally significant effect of fabrication temperature-influenced porosity effects within a 230°C to 290°C range on the tensile performance of AM fabricated CF-PA composite was observed. This is in line with the CT scan microscopy results in section 3.2.1 which showed the overall porosity to reduce as much as 38% from 230 °C to 290 °C for the samples investigated. Figure 9 shows the different mechanical properties examined for the AM-fabricated CF-PA composite.

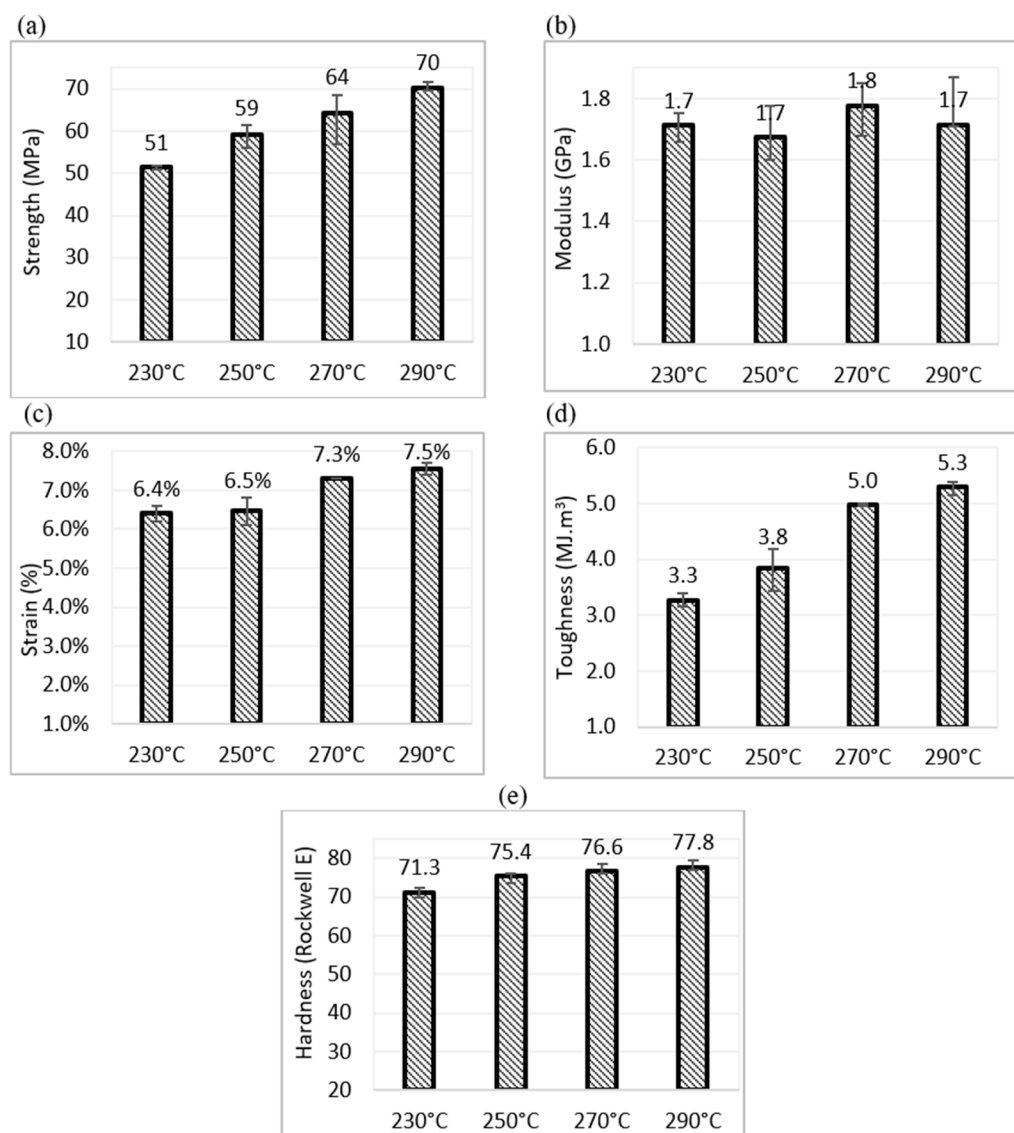


Figure 9. Tensile Properties of Semi-crystalline CF-PA Composites at Different Printing Temperatures (a) Ultimate Tensile Strength (b) Modulus (c) Ductility (d) Toughness (e) Hardness.

Tensile Strength: The material tensile strength properties shown in Figure 9a is an indication of the maximum stress that can be applied while stretched in tension before material failure by elastic or plastic deformation. Printing temperatures played some role in influencing tensile strength which can be related to the interlayer porosity feature as seen with the mesostructure formation and micro CT scan evaluation in sections 3.1.1 and 3.2.1, respectively. A significant effect was found for the fabricated CF-PA composite, recording up to 37% increase in tensile strength at an optimized 290 °C printing temperature compared to the 230°C baselines.

Fabrication temperature effects can be explained with better fiber-matrix and layer-to-layer molecular bonding with higher temperatures, which promotes better inter-laminar and cross-laminar chemical bonding between print layers. This follows the explanation by Brenken et. al [26] that fabrication temperatures have strong effects on the melt viscosity of plastic matrixes for bond formation between adjacent layers. Higher temperatures further from the glass transition temperature promote diffusion-based fusion of adjacent layers after interfaces are established, while lower temperatures usually result in decreased molecular mobility which hinders the molecular diffusion process.

Tensile Modulus: The modulus values define the stiffness properties of the material. As seen in Figure 9b, fabrication temperatures have insignificant effects on the CF-PA

composite. Less than 10% variations were observed in the modulus properties for the 230 °C to 290 °C print temperatures range. The insignificant fabrication temperature effects can be explained by the theory propounded by Vaes and Puyvelde [22] which explained temperature effects in determining material modulus. They discussed modulus as influenced by the heterogenous self-nucleation of the structural crystals of the composite which is influenced by heat transfer, melting, and shear deformations during the fabrication process. However, not seen to have much effect in the 230°C to 290°C temperature range examined.

Tensile Ductility: The ductility property measures the material's characteristics for plastic deformation before fracture. The results in Figure 9c show fabricating temperature trends similar to that observed for tensile strength in Figure 9a. Up to 17% ductility properties increase was observed at the 290 °C print temperature which offered the optimal temperature compared to 230°C temperature. The reduced degree of porosity volumes with increasing fabrication temperatures can be used to explain this increase in ductility with temperature when the materials are subjected to strain.

Tensile Toughness: The composite material's ability to absorb energy and plastically deform without fracturing is provided by its toughness values. As seen in Figure 9d, similar to the strength and ductility properties, fabrication temperature has some significant effects on the toughness properties of the CF-PA composite with an approximate 60% increase in value observed at the highest 290 °C temperature over the 230°C baseline temperature examined. The toughness property generally determined by the material strength and ductility characteristics have similar determining features of material strength and ductility also influencing the toughness properties.

Hardness: The Rockwell hardness number directly relates to the indentation hardness of the material and defines the resistance of a material to localized plastic deformation. Figure 9a shows the Rockwell E values for the CF-PA composite exhibiting similar deposition temperatures related to hardness trends as the other mechanical properties. Though not as significant as the other properties, there was an upward increase in value with increasing deposition temperatures from 230°C to 290°C which can also be related to the decreased porosities with increasing fabrication temperatures up to 290°C.

3.3.2. Mechanical properties of CF-ABS composite

A generally insignificant effect of fabrication temperature-influenced porosity effects within a 230°C to 290°C range on the tensile performance of AM fabricated CF-ABS composite was observed. This is in line with the CT scan microscopy results in section 3.2.2 which showed the overall porosity for the more part to be within the range of 15%, except for the 270°C fabricating temperature which showed a deviated range of up to 43% from the three other temperature data points under examination. Figure 10 shows the different mechanical properties examined for the AM-fabricated CF-ABS composite.

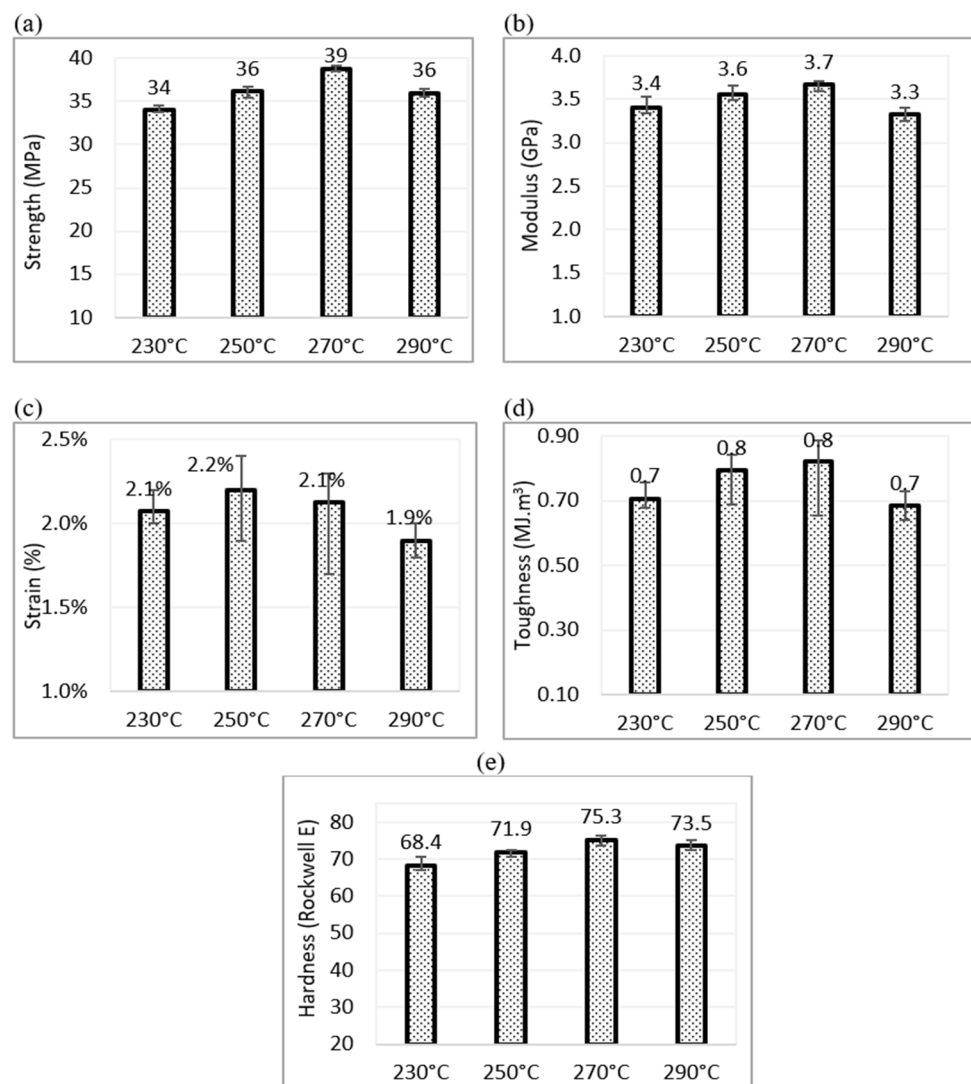


Figure 9. Tensile Properties of Amorphous CF-ABS Composite at Different Printing Temperatures (a) Ultimate Tensile Strength (b) Modulus (c) Ductility (d) Toughness (e) Hardness.

Tensile Strength: As seen in Figure 10a, fabrication temperature played some role in influencing the tensile strength of the CF-ABS composite. However, not so significant. An up to 15% increase in strength was observed at 270 °C found to be optimal for the fabrication temperature range under examination.

Similar to the CF-PA composite, the temperature effects can be explained by the theory of better fiber-matrix and layer-to-layer molecular bonding with higher printing temperatures, due to their promotion of good inter-laminar and cross-laminar chemical bonding between print layers. This similarly follows the explanation by Brenken et. al [26] that fabrication temperatures strongly influence the melt viscosity of plastic matrixes for bond formation between interlayers. High temperatures are needed for the fusion bonding of adjacent beads following interface formation, while lower temperatures usually decrease molecular mobility and limit the molecular diffusion process. However, excessive temperatures can also be detrimental, leading to altering the material composition and degrading the material strength as seen with the CF-ABS composite beyond 270°C fabrication temperature.

Tensile Modulus: As seen with the tensile strength results for the fabricated CF-ABS composite, fabricating temperature has insignificant effects. Figure 10b shows less than 10% variations for the 230 °C to 290 °C fabrication temperatures examined. The insignificant effect on the tensile modulus can be ascribed to the similarity of overall porosity

volumes observed from the CT-scan results which are determinant to the stiffness features which determine the modulus properties of the composite.

Tensile Ductility: As observed for the other tensile properties of the AM fabricated CF-ABS composite, the material ductility as seen in Figure 10c shows similar fabricating temperature effect trends. The effects were found to be insignificant within a 10% range for the 230°C to 290°C fabrication temperatures examined, which can also be attributed to the unsubstantial differences in the overall porosities generated at the fabrication temperatures.

Tensile Toughness: Figure 10d shows the material toughness exhibiting a similar trend as the strength and ductility. Fabrication temperature has an insignificant effect on AM fabricated CF-ABS composite (less than 10%), with the material strength and ductility properties also known to have an overall effect on this property and similar intrinsic material features determining strength and ductility also determining the material toughness characteristics.

Hardness Properties: Similar to the tensile strength, ductility, and toughness, the hardness properties for the AM-fabricated CF-ABS composite as seen in Figure 10a show the Rockwell E values exhibiting similar deposition temperature-related hardness trends. The effect was insignificant but still shows the property value peaking at 270°C also seen for the other tensile properties. The insignificant differences can also be attributed to unsubstantial effects of the deposition temperature on the overall interlayer and intralayer porosity volume differences for the 230°C to 290°C deposition temperatures examined.

4. Conclusions

In this study, deposition temperature-related porosity effects on mechanical properties: strength, modulus, ductility, toughness, and hardness for AM fabricated CFRP composites using semicrystalline CF-PA and amorphous CF-ABS samples were examined. The investigations were conducted by relating deposition temperature trends to mesostructure formation, porosities, and mechanical properties with the following conclusions drawn:

- (1) Deposition temperatures have some effects on porosity volumes in AM-fabricated composites, with semicrystalline CF-PA having a much more significant effect on the amorphous CF-ABS composite.
- (2) The degree of porosity is largely determined by the characteristics of the matrix material.
- (3) A direct relationship exists between the composite porosity and mechanical properties.
- (4) The overall porosity volumes are determinants of the interlayer and intralayer voids, but the interlayer voids play more role in determining the mechanical properties.
- (5) Semicrystalline composites exhibit higher porosity volumes than amorphous composites due to rapid recrystallization as the chains rearrange during the cooling of the print beads.

Author Contributions: Conceptualization, OA; methodology, OA and NO; validation, OA; formal analysis, OA, and NO; investigation, OA and NO; resources, OA, MR and WC; data curation, OA and NO; writing—original draft preparation, OA; writing—review and editing, OA, MR, and WC; supervision, WC. All authors have read and agreed to the published version of the manuscript.

Funding: This research received no external funding.

Data Availability Statement: Data used in this research are available upon request in Microsoft txt, doc.x and jpg file formats.

Acknowledgments: In this section, you can acknowledge any support given which is not covered by the author contribution or funding sections. This may include administrative and technical support, or donations in kind (e.g., materials used for experiments).

Conflicts of Interest: The Author(s) declare(s) that there is no conflict of interest.

References

1. Frketic, J.; Dickens, T.; Ramakrishnan, S. Automated Manufacturing and Processing of Fiber-Reinforced Polymer (FRP) Composites: An Additive Review of Contemporary and Modern Techniques for Advanced Materials Manufacturing. *Addit Manuf* **2017**, *14*, 69–86, doi:10.1016/j.addma.2017.01.003.
2. Melchels, F.P.W.; Feijen, J.; Grijpma, D.W. A Review on Stereolithography and Its Applications in Biomedical Engineering. *Biomaterials* **2010**, *31*, 6121–6130, doi:10.1016/j.biomaterials.2010.04.050.
3. Dimas, L.S.; Buehler, M.J. Modeling and Additive Manufacturing of Bio-Inspired Composites with Tunable Fracture Mechanical Properties. *Soft Matter* **2014**, *10*, 4436–4442, doi:10.1039/c3sm52890a.
4. Mazzoli, A. Selective Laser Sintering in Biomedical Engineering. *Med Biol Eng Comput* **2013**, *51*, 245–256, doi:10.1007/s11517-012-1001-x.
5. Zhang, W.; Cotton, C.; Sun, J.; Heider, D.; Gu, B.; Sun, B.; Chou, T.W. Interfacial Bonding Strength of Short Carbon Fiber/Acrylonitrile-Butadiene-Styrene Composites Fabricated by Fused Deposition Modeling. *Compos B Eng* **2018**, *137*, 51–59, doi:10.1016/j.compositesb.2017.11.018.
6. Tekinalp, H.L.; Kunc, V.; Velez-Garcia, G.M.; Duty, C.E.; Love, L.J.; Naskar, A.K.; Blue, C.A.; Ozcan, S. Highly Oriented Carbon Fiber-Polymer Composites via Additive Manufacturing. *Compos Sci Technol* **2014**, *105*, 144–150, doi:10.1016/j.comp-scitech.2014.10.009.
7. Ning, F.; Cong, W.; Qiu, J.; Wei, J.; Wang, S. Additive Manufacturing of Carbon Fiber Reinforced Thermoplastic Composites Using Fused Deposition Modeling. *Compos B Eng* **2015**, *80*, doi:10.1016/j.compositesb.2015.06.013.
8. Adeniran, O.; Cong, W.; Bediako, E.; Aladesanmi, V. Additive Manufacturing of Carbon Fiber Reinforced Plastic Composites: The Effect of Fiber Content on Compressive Properties. *Journal of Composites Science* **2021**, *5*, 325, doi:10.3390/jcs5120325.
9. Petrò, S.; Reina, C.; Moroni, G. X-Ray CT-Based Defect Evaluation of Continuous CFRP Additive Manufacturing. *J Nondestr Eval* **2021**, *40*, 1–9, doi:10.1007/s10921-020-00737-7.
10. Tagscherer, N.; Schromm, T.; Drechsler, K. Foundational Investigation on the Characterization of Porosity and Fiber Orientation Using XCT in Large-Scale Extrusion Additive Manufacturing. *Materials* **2022**, *15*, doi:10.3390/ma15062290.
11. Adeniran, O.; Cong, W.; Aremu, A.; Oluwole, O. Forces in Mechanics Finite Element Model of Fiber Volume Effect on the Mechanical Performance of Additively Manufactured Carbon Fiber Reinforced Plastic Composites. *Forces in Mechanics* **2023**.
12. Adeniran, O. Mechanical Performance of Carbon Fiber Reinforced Plastic Composites Fabricated by Additive Manufacturing, Texas Tech University, 2022.
13. Ning, F.; Cong, W.; Hu, Z.; Huang, K. Additive Manufacturing of Thermoplastic Matrix Composites Using Fused Deposition Modeling: A Comparison of Two Reinforcements. *J Compos Mater* **2017**, *51*, 3733–3742, doi:10.1177/0021998317692659.
14. Ning, F.; Cong, W.; Hu, Y.; Wang, H. Additive Manufacturing of Carbon Fiber-Reinforced Plastic Composites Using Fused Deposition Modeling: Effects of Process Parameters on Tensile Properties. *J Compos Mater* **2017**, *51*, 451–462, doi:10.1177/0021998316646169.
15. Ajinjeru, C.; Kishore, V.; Lindahl, J.; Sudbury, Z.; Hassen, A.A.; Post, B.; Love, L.; Kunc, V.; Duty, C. The Influence of Dynamic Rheological Properties on Carbon Fiber-Reinforced Polyetherimide for Large-Scale Extrusion-Based Additive Manufacturing. *International Journal of Advanced Manufacturing Technology* **2018**, *99*, 411–418, doi:10.1007/s00170-018-2510-z.

16. Ajinjeru, C.; Kishore, V.; Liu, P.; Lindahl, J.; Hassen, A.A.; Kunc, V.; Post, B.; Love, L.; Duty, C. Determination of Melt Processing Conditions for High Performance Amorphous Thermoplastics for Large Format Additive Manufacturing. *Addit Manuf* **2018**, *21*, 125–132, doi:10.1016/j.addma.2018.03.004.
17. Kishore, V.; Ajinjeru, C.; Nycz, A.; Post, B.; Lindahl, J.; Kunc, V.; Duty, C. Infrared Preheating to Improve Interlayer Strength of Big Area Additive Manufacturing (BAAM) Components. *Addit Manuf* **2017**, *14*, 7–12, doi:10.1016/j.addma.2016.11.008.
18. Cinquin, J.; Chabert, B.; Chauchard, J.; Morel, E.; Trotignon, J.P. Characterization of a Thermoplastic (Polyamide 66) Reinforced with Unidirectional Glass Fibres. Matrix Additives and Fibres Surface Treatment Influence on the Mechanical and Viscoelastic Properties. *Composites* **1990**, *21*, 141–147, doi:10.1016/0010-4361(90)90006-I.
19. Yang, C.; Tian, X.; Liu, T.; Cao, Y.; Li, D. 3D Printing for Continuous Fiber Reinforced Thermoplastic Composites: Mechanism and Performance. *Rapid Prototyp J* **2017**, *23*, 209–215, doi:10.1108/RPJ-08-2015-0098.
20. Ajinjeru, C.; Kishore, V.; Liu, P.; Lindahl, J.; Hassen, A.A.; Kunc, V.; Post, B.; Love, L.; Duty, C. Determination of Melt Processing Conditions for High Performance Amorphous Thermoplastics for Large Format Additive Manufacturing. *Addit Manuf* **2018**, *21*, 125–132, doi:10.1016/j.addma.2018.03.004.
21. Adeniran, O.; Cong, W.; Aremu, A. Material Design Factors in the Additive Manufacturing of Short Carbon Fiber Reinforced Plastic Composites: A State-of-the-Art-Review. *Advances in Industrial and Manufacturing Engineering* **2022**, *5*, 100100, doi:doi.org/10.1016/j.aime.2022.100100.
22. Vaes, D.; van Puyvelde, P. Semi-Crystalline Feedstock for Filament-Based 3D Printing of Polymers. *Prog Polym Sci* **2021**, *118*, doi:10.1016/j.progpolymsci.2021.101411.
23. Jiang, Z.; Diggle, B.; Tan, M.L.; Viktorova, J.; Bennett, C.W.; Connal, L.A. Extrusion 3D Printing of Polymeric Materials with Advanced Properties. *Advanced Science* **2020**, *7*, 1–32, doi:10.1002/advs.202001379.
24. Gofman, I. v.; Yudin, V.E.; Orell, O.; Vuorinen, J.; Grigoriev, A.Y.; Svetlichnyi, V.M. Influence of the Degree of Crystallinity on the Mechanical and Tribological Properties of High-Performance Thermoplastics over a Wide Range of Temperatures: From Room Temperature up to 250°C. *Journal of Macromolecular Science, Part B: Physics* **2013**, *52*, 1848–1860, doi:10.1080/00222348.2013.808932.
25. Adeniran, O.; Cong, W.; Bediako, E.; Adu, S.P. Environmental Affected Mechanical Performance of Additively Manufactured Carbon Fiber-Reinforced Plastic Composites. *J Compos Mater* **2022**, *56*, doi:10.1177/00219983211066548.
26. Brenken, B.; Dissertation, A. *EXTRUSION DEPOSITION ADDITIVE MANUFACTURING OF FIBER REINFORCED SEMI-CRYSTALLINE POLYMERS*; 2017;